Interaction of atomic hydrogen with the diamond C(111) surface studied by infrared-visible sum-frequency-generation spectroscopy

R. P. Chin, J. Y. Huang, and Y. R. Shen
Department of Physics, University of California, Berkeley, California 94720
and Material Science Division, Lawrence Berkeley Laboratory, Berkeley, California 94720

T. J. Chuang
Institute of Atomic and Molecular Sciences, Academia Sinica, P.O. Box 23-166, Tapei, Taiwan

H. Seki
IBM Almaden Research Center, 650 Harry Road, San Jose, California 95120-6099
(Received 10 May 1995)

Atomic hydrogen (deuterium) adsorbed onto the diamond C(111) surface has been studied by infrared-visible sum-frequency-generation spectroscopy. Monohydride termination of H/C(111) is confirmed by the observation of sharp CH stretch (2838 cm^{-1}) and CH bend (1331 cm^{-1}) modes in the spectrum. Deuterium on the surface gives a CD stretch frequency of 2115 cm^{-1}. The rate of hydrogen adsorption is measured in comparison with the rate of deuterium abstraction by hydrogen. Measurement of thermal desorption of hydrogen from C(111) suggests a near first-order desorption kinetics with an activation energy of 4.0 ± 0.4 eV and a preexponential factor of $10^{15\pm2}$ s^{-1}. On the bare reconstructed C(111) surface, distinct CC surface phonon features characteristic of the (2×1)-reconstructed surface are seen, which seem to support the modified Pandey model of Bechstedt and Reichardt.

I. INTRODUCTION

Diamond thin-film growth by chemical vapor deposition (CVD), using thermal or plasma activation of gas phase species, has proven to be successful and attracted a great deal of attention.[1] Although the conditions leading to good diamond growth are generally known, the detailed mechanisms are not yet clear. To improve the quality of CVD diamond films, especially for electronics applications, a good understanding of the diamond growth process is needed. For this, we must know what and how different reactive species appear on the diamond surface at various stages of the growth process, and how they depend on the surface orientation. We also need to learn how these species adsorb, desorb, and react. Most works reported in the literature have focused on gas composition and gas phase reactions in the CVD process. The results obtained could only provide indirect information about species and their reactions on the surface. Clearly, for a better study of the process, an *in situ* monitoring of the surface with surface vibrational spectroscopy is most desirable. Indeed, electron-energy-loss spectroscopy (EELS) and more recently, sum-frequency-generation (SFG) and Fourier transform infrared (FTIR) spectroscopies have been employed for this purpose.

Atomic hydrogen adsorption on diamond seems to be a very important intermediate step in the diamond growth process. In the hot filament method of growth, for example, hydrocarbon gas is usually heavily diluted with hydrogen (such as $<1\%$ CH_4 in H_2) before passing through a hot filament and impinging on a high-temperature substrate ($\sim850\,^{\circ}C$).[2] This large fractional amount of hydrogen is found to be necessary in producing high-quality diamond films. It is believed that atomic hydrogen facilitates diamond growth by promoting the sp^3 hybridization of carbon, opening reactive sites, and removing graphitic materials. Thus a study of hydrogen adsorption on diamond surfaces is paramount to the understanding of CVD diamond growth.

Several spectroscopic methods have been used to study diamond surfaces and hydrogen adsorption on diamond. Waclawski *et al.*[3] first used high-resolution electron-energy-loss spectroscopy (HREELS) to obtain the vibrational spectrum of an as-polished C(111) surface, and concluded that the surface was terminated by CH_3. Lee and Apai[4] studied hydrogen adsorption on C(111). From their HREELS spectra, they identified the presence of surface phonons on the bare reconstructed C(111) surface, and suggested a plethora of different hydrogen termination for hydrogen adsorption on C(111). Aizawa *et al.*[5] used HREELS to study the C(111) surface of diamond homoepitaxially grown by chemical vapor deposition (CVD) under microwave plasma-assisted deposition conditions. They interpreted the spectrum as due to the presence of CH_3 termination on the surface. In other cases, Hamza, Kubiak, and Stulen[6] used time-of-flight mass spectrometry to study desorption of hydrogen from C(111) and C(100) and the resulting surface reconstruction. Mitsuda *et al.*[7] used low-energy electron diffraction (LEED), Auger, and x-ray photoemission (XPS) to study C(111) surface reconstruction with H adsorption. They showed that only a small hydrogen coverage ($\sim5\%$ ML) is already sufficient to convert the surface to the (1×1) bulk-terminated geometry. We recently used SFG (Ref.

8) to obtain vibrational spectra of hydrogen adsorption on C(111), and found a single peak in the CH stretch region, indicating the presence of only a single monohydride species on the surface. This has been confirmed by the work of Hamza, Kubiak, and Stulen using electron-stimulated desorption ion angular distribution (ESDIAD), and by Butler[9] using surface Fourier transform infrared spectroscopy (FTIR).

All these experiments seem to be consistent with the following picture: hydrogen appears to terminate the as-polished or atomic-hydrogen-dosed C(111) surface; the (1×1) bulk termination stabilizes the surface at sufficiently low temperatures (<1150 K); upon hydrogen desorption at high temperatures (>1450 K), the surface undergoes a reconstruction to the (2×1) geometry. The form of the hydrogen termination, however, still remains a controversy. Some studies suggest the domination of monohydride surface species, while others advocate the presence of other hydride species such as aliphatic $CH_{X=2,3}$ or olefine CH_2. Sample preparation, dosing conditions, surface cleanliness, and limitations of individual spectroscopic techniques may be the cause of these discrepancies. Small sizes of diamond often limit the sensitivity of electron spectroscopies, thermal desorption spectrometry, and FTIR studies. HREELS as a vibrational spectroscopy has the advantage of a wide energy range and good sensitivity, but suffers from relatively poor resolution. Conversely, FTIR has good resolution but poor surface sensitivity.

Infrared-visible sum-frequency generation (SFG), with unique capabilities for surface vibrational spectroscopy, has recently been demonstrated to be a versatile surface probe.[10] Being a second-order nonlinear optical process, it is highly surface sensitive at the interfaces of centrosymmetric bulk media. In addition, it has a transform-limited spectral resolution and a spectral range limited only by the infrared source. The polarization dependence of the spectrum permits deduction of molecular orientations of surface species. It is clear that the technique possesses enough desired advantages for studying hydrides on the diamond surface and resolving the above-mentioned controversy. This *in situ* technique can also be adapted to realistic growth conditions in which the electron spectroscopies are generally inapplicable.

Here we report our recent studies of the interaction of atomic hydrogen on the diamond C(111) surface using SFG spectroscopy. Section II discusses how the surface nonlinear susceptibility contributes to the observed signal, and how information about H/C(111) can be derived. Section III describes the experimental apparatus and sample preparation. Section IV presents experimental results for the hydrogen-terminated surface, the adsorption/abstraction/desorption of hydrogen, and the reconstructed surface, and their respective interpretations are given in Sec. V.

II. SURFACE SUM-FREQUENCY SUSCEPTIBILITY

Infrared-visible SFG as a surface vibrational spectroscopic techniques has been described in earlier publications.[11,12] This second-order process, in the electric-dipole approximation, is forbidden in the bulk of centrosymmetric media but is allowed at its interfaces where the symmetry is necessarily broken. In the case of a monolayer of adsorbates on a centrosymmetric substrate, the macroscopic nonlinear surface susceptibility $\chi_S^{(2)}$ of this layer can be related to the nonlinear molecular polarizability $\alpha^{(2)}$ by a coordinate transformation from the molecular axes denoted by $\hat{l}$, $\hat{m}$, and $\hat{n}$ to the lab axes denoted by $\hat{i}$, $\hat{j}$, and $\hat{k}$:

$$\chi_{S,ijk}=N_S\sum_{l,m,n}\langle(\hat{i}\cdot\hat{l})(\hat{j}\cdot\hat{m})(\hat{k}\cdot\hat{n})\rangle\alpha^{(2)}_{lmn}$$
$$=N_S\langle\alpha^{(2)}\rangle_{ijk} \tag{1}$$

if interactions between molecules are neglected, where N_S is the surface molecular density, and the angular brackets $\langle\ \rangle$ denote the orientational average. The nonzero independent elements of $\chi_S^{(2)}$ (we will omit the S from now on for brevity) can be deduced by measuring the signals for different polarizations of the incident and output beams.

Consider for example, a (111) surface with a $C_{3v}(3m)$ symmetry lying in the XY plane and having the mirror plane in XZ. It should have five independent surface nonlinear susceptibility elements: the anisotropic terms $\chi^{(2)}_{YYX}=\chi^{(2)}_{YXY}=\chi^{(2)}_{XYY}=-\chi^{(2)}_{XXX}$, and the isotropic terms $\chi^{(2)}_{ZYY}=\chi^{(2)}_{ZXX}$, $\chi^{(2)}_{YYZ}=\chi^{(2)}_{XXZ}$, $\chi^{(2)}_{YZY}=\chi^{(2)}_{XZX}$, and $\chi^{(2)}_{ZZZ}$. The subindices here refer to the directions of the field components of the sum-frequency output, visible input, and infrared input, respectively. If we now choose the plane of incidence to coincide with the YZ plane and the output/input polarization combination as *pss* (sum-frequency output, visible input, and infrared input, *p*-, *s*-, and *s*-polarized, respectively), we can deduce from the SFG measurement the element $\chi^{(2)}_{ZXX}$. With the *ssp*, *sps*, and *sss* combinations, we can readily obtain $\chi^{(2)}_{XXZ}$, $\chi^{(2)}_{XZX}$, and $\chi^{(2)}_{XXX}$, respectively. Finally, the *ppp* combination, we can find $\chi^{(2)}_{ZZZ}$ from the SFG measurement, knowing $\chi^{(2)}_{XXZ}$, $\chi^{(2)}_{XZX}$, and $\chi^{(2)}_{XXX}$.

The effective surface susceptibility for the SFG process near vibrational resonances can usually be written as the sum of a resonant term $\chi_R^{(2)}$ and a nonresonant term $\chi^{(2)}_{\rm NR}$:[13]

$$\vec{\vec{\chi}}^{(2)}_S=\vec{\vec{\chi}}^{(2)}_{\rm NR}+\vec{\vec{\chi}}^{(2)}_R\ ,$$
$$\vec{\vec{\chi}}^{(2)}_R=N_S\sum_Q\langle\vec{\vec{\alpha}}^{(2)}\rangle_Q$$
$$=N_S\sum_Q\left\langle\frac{\vec{\vec{A}}_Q}{\omega_{\rm IR}-\omega_Q+i\gamma_Q}\right\rangle\ , \tag{2}$$

where $\mathbf{A}_Q=\langle g|\boldsymbol{\mu}|n\rangle\langle n|\mathbf{M}|g\rangle/\hbar$. Here Q refers to the resonance mode with its frequency and damping constant denoted by ω_Q and γ_Q, and its contribution to the SFG is proportional to A_Q, which is a product of the infrared dipole matrix element $\langle g|\mu_k|n\rangle$ term and the Raman matrix element $\langle n|\mathbf{M}|g\rangle$. With the SF output proportional to $|\chi_S^{(2)}|^2$, the resonant enhancement of $\chi_S^{(2)}$ as $\omega_{\rm IR}$ scans over ω_Q yields the desired surface vibrational spectrum.

To see how the determination of $\chi^{(2)}_{R,ijk}$ can yield infor-

mation about the orientation of a molecular or a bond at a surface, we consider the stretch mode of a carbon monohydride (CH) distributed isotropically on a surface. We can relate the relevant elements of $\chi_R^{(2)}$ to the molecular polarizability $\alpha_{\xi\xi\xi}^{(2)}$ of the CH bond by

$$\chi_{R,YYZ}^{(2)}=N_S\alpha_{\xi\xi\xi}^{(2)}[\tfrac{1}{2}(1-r)\langle\sin^2\theta\cos\theta\rangle+r\langle\cos\theta\rangle]\ ,$$
$$\chi_{R,YZY}^{(2)}=\chi_{R,ZYY}^{(2)}=\frac{N_S}{2}\alpha_{\xi\xi\xi}^{(2)}(1-r)\langle\sin^2\theta\cos\theta\rangle\ , \quad (3)$$
$$\chi_{R,YYX}^{(2)}=\chi_{R,YXY}^{(2)}=\chi_{R,XYY}^{(2)}=0\ ,$$

where θ is the orientation angle of the CH relative to the surface normal, $r=\alpha_{\eta\eta\zeta}^{(2)}/\alpha_{\xi\xi\xi}^{(2)}$ (≈ 0.14) is the ratio of transverse and longitudinal Raman polarizability associated with a CH bond,[14] η and ζ are the axes perpendicular and parallel to the bond axis, respectively, and $\langle\ \rangle$ denotes the orientational average of the CH bonds on the surface. From Eq. (3), it is now possible to determine the polar bond angle (assuming an orientational distribution) from $\chi_{R,YYZ}^{(2)}$ and $\chi_{R,YZY}^{(2)}$.

For the bare, reconstructed surface C(111)-(2×1), the π-bonded chains are aligned along the (2×1) domains. With such domains oriented in three equivalent directions, the surface is sometimes referred as the C(111)-(2×1)/(2×2) surface. For this reconstructed surface, a particular bond with azimuthal angle ϕ has a matching bond with an opposite azimuthal angle $-\phi$, thereby effectively yielding azimuthal isotropy with $\chi_{R,YYX}^{(2)}=0$.

In a similar manner, the terms for the CH bending mode can be derived using Eq. (1). Further, other hydride configurations, such as for aliphatic CH_2 and CH_3, and olefinic $=CH_2$, can also be derived.

III. EXPERIMENTAL APPARATUS AND SAMPLE PREPARATION

The experimental setup has been described elsewhere.[11,12] In the present experiment, the laser system produces picosecond visible (0.532 μm, 17 ps) and tunable infrared pulses for the SFG experiment. Tunable infrared pulses (~17 ps) at ~3.5 μm with a 12-cm^{-1} linewidth were generated from a $LiNbO_3$ optical parametric generator/amplifier (OPG/OPA) producing 400–500 μJ per pulse at 15 pulses per second. A second, more sophisticated barium borate (BBO) OPG/OPA seeding a $AgGaS_2$ difference frequency generation (DFG) system generated broadly tunable (~8 ps) infrared pulses (3.5–10 μm) with 100 μJ at ~5 μm and ~50 μJ at ~7 μm, with a 4-cm^{-1} linewidth.[15] The visible and infrared beams were overlapped on the diamond surface with beam diameters of ~600 and ~300 μm, respectively. A 7° angular separation between the input beams (46° for the visible and 53° for the infrared beam) permitted spatial separation of the second-harmonic and sum-frequency output signals as determined by the phase-matching conditions. Both signals were simultaneously measured with separate detection arms using sensitive gated photon-counting techniques. Polarization combinations normally used for SFG were: *ssp* (*s*-polarized SFG, *s*-polarized visible, *p*-polarized IR), *pss*, *ppp*, and *sps*.

The tunable infrared sources were calibrated to within 2 cm^{-1} with polystyrene/mica references and a calibrated monochromator. All SFG spectra were normalized against a nonresonant SFG signal from, for example, a crystalline quartz to minimize effects due to IR energy changes, beam overlap variations, and detector responsivity during scans. The peak positions (ω_q), strengths (A_q), and widths (γ_q) of $\chi_R^{(2)}$ and the nonresonant background $\chi_{NR}^{(2)}$ were determined by a fit of the SFG spectrum to Eq. (2).[13]

A natural type-IIa diamond cut to within 3° of the (111) surface was mechanically polished with 0.25-μm diamond abrasive in olive oil to produce a hydrogen-saturated surface.[16] Cleaning was accomplished using an acid bath (one part HNO_3, three parts H_2SO_4 at 100 °C for 10–20 h), followed by a rinse in distilled water and then in methanol. The sample was mounted on an all-molybdenum resistive heater within an ultrahigh-vacuum chamber with a base pressure of $\sim 5\times10^{-10}$ torr. No tantalum metal was used, as this had been found to cause a substantial contamination on diamond especially with hydrogen adsorption. During the bakeout, the sample was kept at 500 °C to keep the sample clean and to outgas the heater. The sample temperature was measured using a 0.005-in. ϕ type-G thermocouple in intimate contact with the diamond but not with the heater. A 1800 °C (5 mm×10 mm×0.001 in.) tungsten filament,[17] 12–16 mm from the diamond surface, was used to dissociate molecular hydrogen for atomic hydrogen dosing. The sample during dosing was initially at room temperature but rose to ~200 °C after an extended period of dosing (>30 min) due to radiative heating. An optical pyrometer reading, compensated for emissivity and viewport biases, was used to determine the hot filament temperatures. The pressure of H_2 for dosing was typically 5×10^{-7}–1×10^{-5} torr. The dosing setup and procedure were the same as those used in our x-ray photoemission spectroscopy (XPS), Auger electron spectroscopy (AES) thermal-desorption spectroscopy (TDS), and LEED studies.[7]

We will focus on the SFG spectra (*ssp*) associated with $\chi_{YYZ}^{(2)}$ in the CH stretch region because this arrangement yields the strongest SFG signal from a hydrogen-saturated C(111)-(1×1)-H surface.[8] For the H-terminated surface, a single CH stretch peak was observed. With the sample mildly annealed at ~600 °C, the peak became slightly narrower (~6–10-cm^{-1} FWHM) and stronger by 10–50%. If the sample was dosed at ~800–850 °C with $\sim 1\times10^{-5}$ torr H_2 for 5–10 min and then stopped at a 750 °C substrate temperature as the sample quickly cooled, a stronger and narrower peak signal was immediately attained. This latter procedure was extremely effective at reliably reproducing a well-prepared H-terminated C(111) surface characterized by a single, strong, and narrow CH stretch peak. Once hydrogen terminated, the signal remained unchanged after 20 h of storage in vacuum ($<10^{-9}$ torr). By heating the sample to 1500 K, all H atoms were desorbed and the surface was reconstructed to form (2×1). The cycle of H dosing to restore the (1×1) structure and the desorption of all H to form (2×1) were completely reproducible.[7]

IV. EXPERIMENTAL RESULTS

A. Hydrogen-terminated surface C(111)-(1×1)-H

A clean, well-ordered C(111)-(1×1)-H surface should exhibit a simple truncated bulk structure.[6,7,16] The monohydride surface layer is expected to yield a single CH stretch mode and a single CH bend mode. In our earlier study,[8] the *ssp* SFG spectrum of a H-saturated C(111) surface indeed showed a *single* CH stretch peak at $\sim$2830 cm^{-1}. Using our narrow-linewidth, better calibrated, and more broadly tunable infrared source, from the *ssp* SFG spectrum we now obtained a single stretch peak[18] at 2838 cm^{-1} and a *single* CH bending mode peak at 1331 cm^{-1} (Fig. 1). For the *sps* spectrum, the bending mode peak was strong but the stretch mode peak was essentially absent. No other spectral features were discernible in the range of 1100–3300 cm^{-1}. These results are expected from the on-top adsorption of H on C(111). It is coincidental that this has nearly the same frequency as the zone-center phonon mode of the substrate (1332.5 cm^{-1}),[19] as determined by Raman spectroscopy. To be sure that our observed peak at 1331 cm^{-1} was indeed the CH bending mode, we dosed the surface with deuterium to replace hydrogen. We found that the 1331-cm^{-1} peak was completely suppressed as the CD bending mode should appear at $\sim$900 cm^{-1} instead, and the corresponding CH stretch peak at 2838 cm^{-1} was replaced by the CD stretch peak at 2115 cm^{-1}. The latter is presented in Fig. 2 for a C(111) surface saturated by deuterium. The observed CD stretch frequency (2115 cm^{-1}) is about 0.75 times the CH stretch frequency (2838 cm^{-1}). This can be compared with the approximate theoretical ratio of $1/\sqrt{2}=0.71$, the ratio of 0.75 for *DC* Cl_3 (2255 cm^{-1}) versus *HC*Cl_3 (3019 cm^{-1}),[20] and the ratio of 0.71 for *DC*$(CD_3)_3$ (2063 cm^{-1}) versus *HC*$(CD_3)_3$ (2887 cm^{-1}).[21]

As previously reported,[8] the beam polarization dependence of the stretch peak gives information about the orientation of the CH bond. The observation that the *p*-polarized infrared light could excite the CH stretch more strongly than the *s*-polarized infrared light indicates that the CH bond is lying preferentially along the surface normal. Our analysis yielded a 30° distribution about the surface normal. A similar analysis for the bending mode yielded nearly equal intensities for *s*- and *p*-polarized infrared beams, as the dipole moment is now parallel to the surface.

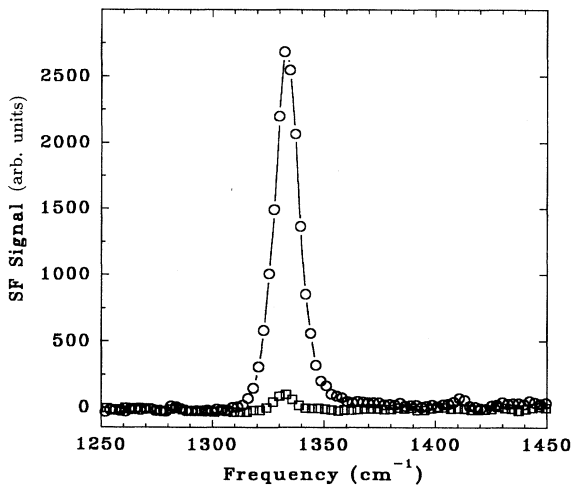

FIG. 1. SFG spectra of the H-terminated H/C(111)-(1×1) surface showing the CH bending mode (open circles) and the same surface dosed with atomic deuterium (open squares). Both curves are for *ssp* polarization geometry.

B. Temperature dependence of the CH stretch frequencies and linewidths

Our experimental apparatus only allowed heating of the sample above room temperature. We were able to take high-temperature SFG spectra of the hydrogen-dosed C(111) surface for both the CH stretching and bending modes. Figure 3 depicts two spectra at 300 and 700 K. Both modes exhibit a temperature-dependent shift in the peak position and broadening of the peak width. For the CH bend and stretch modes, the peak positions change from 1330 to 1324 cm^{-1} and from 2837 to 2833 cm^{-1}, respectively, as the temperature increases from 300 to 700 K, while the corresponding peak half-widths change from 5 to 7 cm^{-1} and from 7 to 9 cm^{-1}, respectively. The half-widths were deconvoluted from the data in Fig. 2 with a 4.5-cm^{-1} (FWHM) Gaussian infrared laser line shape.

The increase of peak widths with temperature suggests that the peaks are homogeneously broadened. This is supported by the CD spectrum in which the CD stretch peak exhibits a $\sim$40 cm^{-1} half-width. Since the chemical environment (i.e., the chemical structure and binding) should be the same for this isotopic H→D substitution, the change (increase) in the linewidth cannot be attributed to inhomogeneous broadening. It is most probable that the linewidth is dominated by dephasing broadening.

C. Adsorption, desorption, and abstraction of hydrogen

Second-harmonic generation (SHG) can be used to follow the response of the bare reconstructed diamond (111)

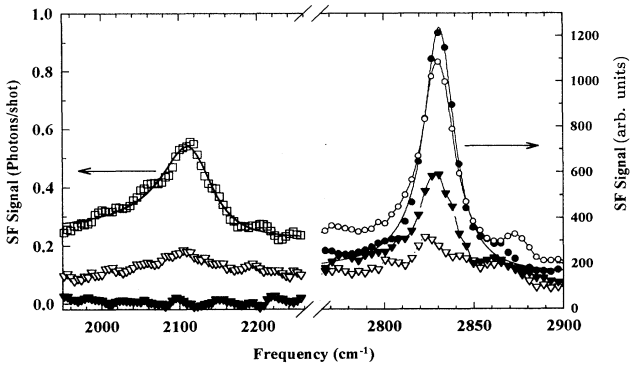

FIG. 2. SFG spectra (*ssp*) showing gradual replacement of D by H upon atomic H dosing onto the fully D-terminated surface. Full D coverage (open squares), 3-min H dosing (open triangles), 8-min H dosing (solid triangles), 13-min H dosing (open circles), and 18-min H dosing (solid circles).

surface to atomic hydrogen dosing.[7] In our previous study, the SHG signal during atomic H dosing responded to H adsorption on the surface and the phase transition of the (2×1)-reconstructed surface to the unreconstructed (1×1) surface. The latter was observed to occur with only ~5% ML hydrogen coverage.

SFG spectra for different hydrogen coverages resulting from hydrogen dosing and thermal desorption have also been reported earlier.[8] During H adsorption, a metastable peak at ~2865 cm^{-1} (corrected from 2860 cm^{-1} as reported in Ref. 8) was observed for coverages less than ~0.5 ML, but gradually disappeared in favor of the 2838-cm^{-1} peak toward full hydrogen coverage. In contrast, during thermal desorption of hydrogen, only the usual ~2838-cm^{-1} peak with reducing strength was seen.

Atomic hydrogen adsorbs readily to the bare diamond surface. From CVD growth experiments, a large amount of hydrogen is often needed to produce high-quality films. Presumably the stable surface of diamond is mostly covered by hydrogen. We have investigated how hydrogen adsorption and abstraction affect the equilibrium H coverage on the C(111) surface. We used SFG spectroscopy to monitor *in situ* the surface coverages of hydrogen and deuterium when a D-terminated surface was dosed by atomic H, assuming that the binding energies of H and D to the surface are the same.

Figure 3 illustrates the occurrence of H (D) abstraction. As atomic hydrogen was dosed (2×10^{-6}-torr H_2 with the hot filament) onto the deuterium-covered surface, the CD peak at 2115 cm^{-1} decreased in strength while the CH peak at 2838 cm^{-1} increased. After ~10 min, the spectrum was totally dominated by the CH peak. It is apparent that atomic hydrogen was very effective at abstraction. We should note that molecular hydrogen had no effect on either the bare reconstructed surface or the deuterium-terminated surface. Only atomic hydrogen appeared to react with the surface.

From the CH peak strength, we can deduce the H coverage on the surface. Figure 4 shows the surface coverage of H on C(111) at room temperature as a function of

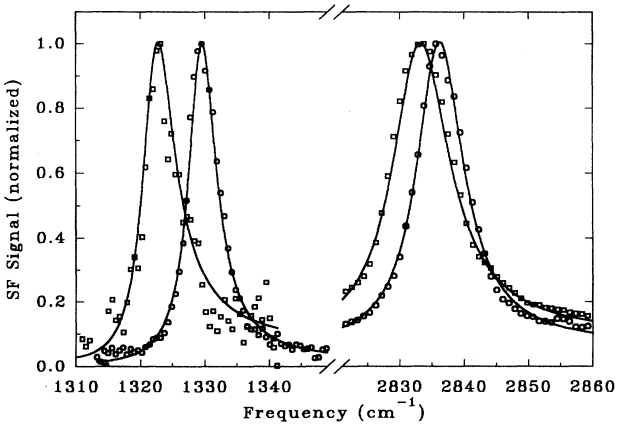

FIG. 3. SFG spectra (*ssp*) of CH bending and stretching modes for H/C(111) at 300 (open circles) and 700 K (open squares).

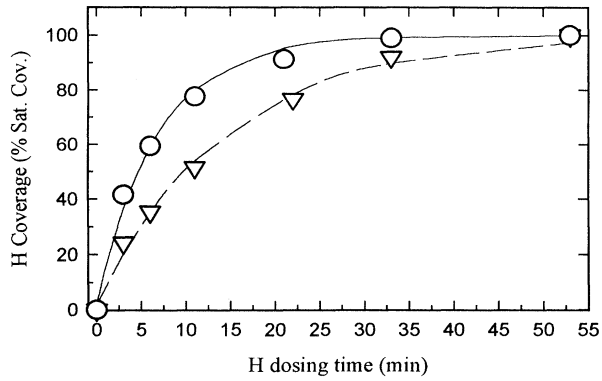

FIG. 4. Surface coverage of H as a function of H dosing time for atomic H dosing onto a bare reconstructed (2×1) surface (open circles) and onto a fully covered deuterium surface (open triangles).

dosing time at a H_2 pressure of 5×10^{-7} torr with atomic hydrogen dosed on a bare reconstructed surface and on a deuterium-covered surface. The adsorption on the bare surface appears to proceed faster than on the deuterium-covered surface as one would expect that the sticking probability of H should be lower for the D-covered surface than the bare or sparsely occupied surface. From the difference in the two rates, we can deduce roughly the ratio of the rate of abstraction K_{abs}, versus the rate of adsorption, K_{ads}. For dosing of the bare surface, the rate of change of the hydrogen coverage (Θ_H) is given by

$$\frac{d\Theta_H}{dt}=K_{ads}(1-\Theta_H)-K_{abs}\Theta_H ,$$
$$\text{At } t=0:\ \Theta_H=0 , \tag{4}$$
$$\text{At } t\to\infty:\ \frac{d\Theta_H}{dt}=0,\ \Theta_H=\Theta_{eq}=\frac{K_{ads}}{K_{ads}+K_{abs}} .$$

For H dosing of the deuterium-covered dosed surface, the rate equations for hydrogen (Θ_H) and deuterium (Θ_D) coverages are

$$\frac{d\Theta_H}{dt}=K_{ads}(1-\Theta_H-\Theta_D)-K_{abs}\Theta_H ,$$
$$\frac{d\Theta_D}{dt}=-K_{abs}\Theta_D ,$$
$$\text{At } t=0:\ \Theta_H(t=0)=0,\ \Theta_D(t=0)=\Theta_D^0<1\text{ ML} , \tag{5}$$
$$\text{At } t\to\infty:\ \frac{d\Theta_H}{dt}=\frac{d\Theta_D}{dt}=0,\ \Theta_H=\Theta_H=\frac{K_{ads}}{K_{ads}+K_{abs}} ,$$
$$\Theta_D=0 .$$

Here we have assumed that the rate of abstraction of deuterium is the same that as for hydrogen.

By fitting the data in Fig. 3 with the above equations, the ratio $K_{abs}/K_{ads}=0.2$ was found. This gives an equilibrium coverage of $\Theta_{eq}=K_{ads}/(K_{ads}+K_{abs})=83\%$ at room temperature. We also find experimentally that the strength of the SFG signal for H-saturated C(111) at 300 K is about 80% of that obtained with the sample at 1000

K. This may be due to the annealing effect on the adsorption and/or an indication that the rate of adsorption to the rate of abstraction is higher at higher temperatures.

D. Determination of the kinetic parameters for thermal desorption of hydrogen

Thermal desorption of H from C(111) can provide information about hydrogen desorption kinetics. In ultrahigh vacuum, with readsorption negligible, desorption of hydrogen can be assumed to obey the equation

$$\frac{d\Theta_{\mathrm{H}}}{dt} = -k_d \Theta_{\mathrm{H}}^n , \tag{6}$$

where n is the order of the reaction, $k_d = \nu \exp(-E_d/k_B T)$, ν is the preexponential factor, E_d is the desorption activation energy (we assume that ν and E_d do not depend on coverage or temperature), k_B is the Boltzmann factor, and T is the temperature which can be a function of time t. If $n > 1$, we can integrate Eq. (6) to yield

$$\frac{1}{(n-1)} \left[\frac{1}{\Theta_f^{n-1}} - \frac{1}{\Theta_f^{n-1}} \right] = \int_{t_1}^{t_1} dt\, \nu \exp(-E_d/k_B T) \quad (n > 1) . \tag{7}$$

We have used SFG to monitor the H coverage (Θ_{H}) following thermal desorption. The measurements were made each time after the surface was rapidly heated to a high goal temperature where desorption was appreciable and cooled back to room temperature (where practically no desorption occurred). The goal temperature of each heating cycle was varied from 700 to 1000 °C. The temperature profile $T(t)$ of each heating cycle was automatically recorded (every 0.5 s). Typically, heating to 800 °C from room temperature required at least ~45 s and cooling to 500 °C required at least ~200 s. For lower goal temperatures (~750 °C), the sample was held at the goal temperature for a longer interval in order to have an appreciable change in the H coverage by thermal desorption.

As reported earlier, the SFG spectrum of the CH stretch would exhibit a complex line-shape change with the H desorption[8] resulting from interference of the resonant background $\chi_R^{(2)}$ with the nonresonant background $\chi_{\mathrm{NR}}^{(2)}$. However, by a fit of the spectrum to Eq. (2), we could deduce $\chi_R^{(2)}$, which is proportional to Θ_{H}. In the desorption measurements, we used the heating cycles described in Fig. 5 (solid lines). Starting with a saturated H coverage (normalized to 1) at the beginning of the first, sixth, and eight cycles, the coverages Θ_{H} were measured and presented in Fig. 5 (open squares). The theoretical fit by Eq. (7) is also shown (dashed lines) in the figure for comparison using the measured temperature profiles $T(t)$ and n, ν, and E_d as fitting parameters. (Cycles 6 and 8 were specifically chosen to desorb at a low temperature, while cycles 4, 5, 7, and 9 were used to include low coverage data. This enabled a more precisely determined fit to the parameters with ν and E_d not strongly interdependent in the fitting.) From the fit for the C(111)-(1×1)-H surface, we obtained $n = 1.3 \pm 0.3$, $\nu = 10^{15\pm2}$ s^{-1}, and $E_d = 4.0 \pm 0.4$ eV. The uncertainty in the parameters reflects the experimental uncertainty in determining the coverage and the temperature.

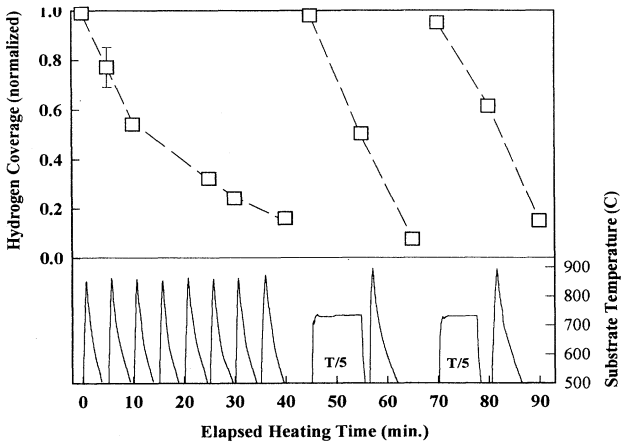

FIG. 5. Variation of surface coverage of H (open squares) in response to the prescribed thermal desorption cycle shown in the lower figure. The dashed lines represent the theoretical fit using Eq. (6).

We can use the desorption energy E_d to estimate the CH bond strength. Assuming E_d is equal to the heat of adsorption, the CH chemical bond energy can be obtained[22] using $2E_{\mathrm{C\text{-}H}} = (E_d + E_{\mathrm{H\text{-}H}})$, since a hydrogen molecule must dissociate with dissociation energy $E_{\mathrm{H\text{-}H}}$ to form two CH bonds with the surface. With $E_{\mathrm{H\text{-}H}} = 4.42$ eV and $E_d = 4.0$ eV, we obtain $E_{\mathrm{C\text{-}H}} = 4.2$ eV, which is about 10% smaller than a typical aliphatic CH bond (~4.5 eV). This is commensurate with the observed lower frequency of the CH stretch mode on C(111) as compared to that of a molecule [such as $CH(CH_3)_3$], indicating a weaker CH bond for H on C(111).

E. Reconstructed C(111)-(2×1) surface

If the C(111)-(1×1)-H surface is heated to >1200 °C, the surface reconstructs to the C(111)-(2×1)/(2×2) surface, as indicated by LEED.[6,7,16] Under the same conditions, we found the complete suppression of the 1331- and 2838-cm^{-1} CH peaks, indicating the disappearance of hydrogen by thermal desorption. In the low-frequency range (1300–1500 cm^{-1}), however, additional peaks appeared (Fig. 6). They must represent the surface phonons of the C(111) surface . It must be emphasized that very little hydrogen (~0.05 ML) is needed to hold the (1×1) phase, and that essentially complete hydrogen desorption must occur to cause the above-described phase transition and the resulting spectra. If a small amount of atomic hydrogen is dosed (~0.05 ML) onto the (2×1)-reconstructed surface, the surface phonon features completely disappear, leaving a featureless spectrum; the CH bending mode is below the detection limit.

SFG is forbidden in the bulk of diamond because of existence of inversion symmetry. Near the H-terminated C(111)-(1×1) surface, although the C—C bonds might experience a broken symmetry, their contribution to SFG

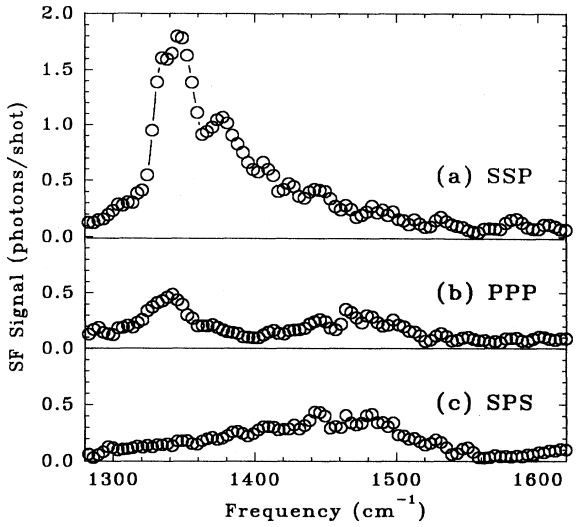

FIG. 6. SFG spectra of the bare, reconstructed C(111)-(2×1) surface for *ssp* (upper curve), *ppp* (middle curve), and *sps* (lower curve) polarization geometries. Spectral features come from C-C surface vibrational modes.

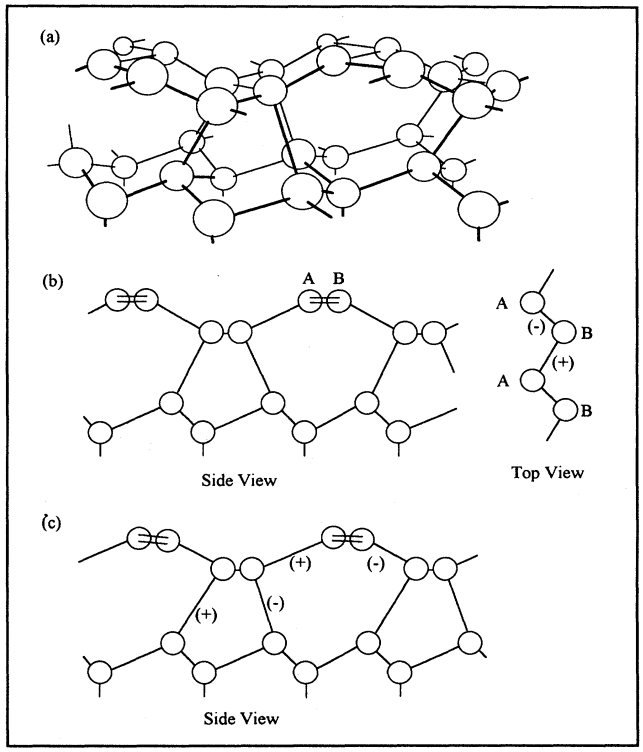

FIG. 7. (a) Schematic representation of the Pandey π-bonded chain model showing the CC bonds. (b) Dimerization (no buckling) in the Pandey π-bonded chain model proposed by Iarlori *et al.* (in Ref. 23). (c) Slight buckling (no dimerization) in the Pandey π-bonded chain model proposed by Bechstedt and Reichardt (in Ref. 23).

was not observed; only the CH bending (1331 cm^{-1}) and stretching (2838 cm^{-1}) modes appeared in the spectrum for H coverages of 0.05–1 ML. However, if hydrogen is fully desorbed, the reconstruction of the diamond surface involves a radical rearrangement of the surface carbon atoms. The current accepted model for the C(111) reconstruction is the Pandey (2×1) π-bonded chain model.[23] This results in a surface structure (Fig. 7) composed of a topmost layer of carbon chains with mostly sp^2 character and a next layer of carbon chains with mostly sp^3 character. This structure is highly asymmetric, allowing its vibrational modes observable by the infrared SFG technique.

Figure 6 shows two major bands of the SFG spectrum of the C(111)-(2×1)-reconstructed surface between 1300 and 1500 cm^{-1}: a low-frequency one around 1350 cm^{-1} observed with the IR input *p*-polarized and a second one 1475 cm^{-1} observed with both *p*- and *s*-polarized IR input. We could in principle deduce the bond orientations from the ratios of the peaks in the *ssp* and *sps* SFG spectra using Eq. (3), and assuming that surface vibrations are localized to bonds. However, for C—C bonds, the transverse polarizabilities are not known making the deduction of the bond orientations difficult.

With some simplifying assumptions, we can still obtain some qualitative information about the bond orientations. From Eq. (3), we find that a ratio $|\chi_{YYZ}/\chi_{YZY}| \approx 1$ would indicate $\Theta \sim 90°$ for $r = \alpha^{(2)}_{\eta\eta\zeta}/\alpha^{(2)}_{\zeta\zeta\zeta} < 0.1$. This is the case for the observed ~1475-cm^{-1} band as seen from Fig. 6, suggesting that the C—C bonds responsible for the band must lie close to the surface plane. For the ~1350-cm^{-1} band, we find, from Fig. 6, $|\chi_{YYZ}/\chi_{YZY}| \approx 3$. If $0 < r < 0.1$ (knowing $r = 0.14$ for CH bonds), we obtain from Eq. (3), $0° < \Theta < 35°$. This indicates that the corresponding C—C bonds must be leaning fairly close along the surface normal. We shall discuss how the picture fits with the surface structure in Fig. 7 in Sec. V.

As seen in Fig. 6, the ~1350-cm^{-1} band is composed of two peaks 30 cm^{-1} apart. The ratios of $|\chi_{YYZ}/\chi_{YZY}|$ for the two peaks are similar. These observations suggest the presence of two types of C—C bonds having nearly the same polar orientation (presumably not far away from the surface normal). For the ~1475-cm^{-1} band, one could regard it as a broad feature with a full width of ~60 cm^{-1}, or also imagine two overlapping peaks with half the full width. In the latter case, the corresponding two types of C—C bonds would both lie nearly flat on the surface.

V. DISCUSSION

A. Hydrogen adsorption, desorption, and abstraction on the C(111) surface

Waclawski *et al.*[3] studied hydrogen adsorption on C(111) using HREELS. They concluded after comparing with the deuterated ethane spectra that $-CH_3$ must have terminated the surface. Their explanation for the presence of CH_3 species rather than the expected CH monohydride included the possibility of surface defects not detected in the (1×1) LEED pattern; the corrosive action hydrogen on diamond to create CH_2 and CH_3, similar to hydrogen on silicon;[24] and the breakup of the

π-bonded chains during the adsorption process, leaving only singly backbonded sp^3 hybridized carbons with the three remaining bonds occupied by hydrogen.

Recently, Lee and Apai[4] similarly used HREELS, except with better resolution, to study hydrogen-terminated and bare (2×1)-reconstructed (111) and (100) surfaces. For surfaces with H adsorption, not only did they assign peaks to CH_3, they also believed in seeing evidence for other aliphatic (sp^3) and olefinic (sp^2) hydrocarbon species. They attributed the plethora of surface coordinations to the crude surface preparation with inherent multiple H-adsorption sites and the propensity for carbon-carbon bond breaking in preference to hydrogen termination as in the case of silicon.[24]

In contrast, our SFG measurements of the as-polished and the atomic hydrogen exposed diamond C(111) surface with much better spectral resolution clearly show a *single* CH stretch at 2838 cm^{-1} and a *single* CH bend at 1331 cm^{-1} with linewidths narrower than 10 cm^{-1} and no other spectral features between 1100 and 3300 cm^{-1}. From the peak frequencies and the mode's polarization dependence, we conclude that this peak must originate from a monohydride CH stretch with H sitting on top of C and not from other aliphatic $CH_{2,3}$ or olefinic CH_2 species.

Our conclusion that H terminates the C(111)-(1×1) surface in the CH monohydride form is consistent with the results of helium scattering and diffraction[25] and proton desorption (ESDIAD).[6] It has been suggested[4] that the discrepancies among works from different laboratories could be due to differences in the diamond samples and sample treatments. Our experience and others[26] with different diamond samples and various sample holding and preparation techniques, show that this is indeed the case. In particular, the use of Ta as a sample holding material may cause severe sample contamination.[4,6] The SFG technique is very surface sensitive, making it ideally suited to distinguish different types of hydrides on the surface and the degree of ordering, as evidenced by the signal strength and linewidth, and, in principle, also the polarization dependence. For the C(111) diamond, consistently high-quality hydrogen-terminated surfaces necessitated the use of an acid bath for extended periods of time in order to remove graphitic carbon after polishing. Residual strain in the diamond sample appearing on the surface after repeated high-temperature heating processes could also cause difficulties, with spectral peaks excessively broadened by inhomogeneous broadening.

In hydrogenating the diamond surface for spectroscopic studies, it has been common to dose atomic hydrogen upon a bare substrate at or near room temperature. We have found that after repeated hydrogen dosing and desorption, the H-terminated surface often became less well ordered, as evidenced by weaker and broader CH peaks and the appearance of features indicative of the presence of other hydrocarbon species. However, if the substrate was dosed by atomic hydrogen at 800–850 °C as well as during cooling to ~750 °C, the resulting H-terminated C(111) surface always appeared well ordered. SFG spectra with strong and narrow CH stretch and bend peaks were observed even if the surface originally had been contaminated, for example, by activated methane, methyl iodide, or tert-butyl peroxide. Presumably, the aggressive replacement of unwanted hydrocarbon or carbon species by preferential hydrogen adsorption on the well-annealed surface is the reason behind the successful surface treatment.

For the well-ordered H-terminated surface, the CH stretch and bend modes exhibited the minimum linewidths, 5 and 7 cm^{-1}, respectively, at room temperature. They are likely dominated by homogeneous broadening resulting from the dephasing (T_2) mechanism. The lifetimes (T_1) of the CH stretch mode have been measured[18] to be ~19 ps, which corresponds to a broadening of only 0.25 cm^{-1}. Inhomogeneous broadening is presumably not of dominant importance because of our observation of temperature broadening of the peaks (from 5 to 7 and 7 to 9 cm^{-1}, respectively, for the stretch and bend modes as the sample temperature changed from 300 to 700 K). Further evidence against inhomogeneous broadening comes from the observation that the CD stretch mode is ~8 times broader than that of CH, while their physical and chemical environments giving rise to the inhomogeneous broadening are expected to be the same. That the CD stretch peak is much broader than the CH stretch can be easily understood knowing that the two-phonon absorption band of diamond[27] is in the range of 2000–2250 cm^{-1}, which resonantly couples with the CD stretch and enhances its dephasing relaxation.

The observed monohydride CH stretch frequency (2838 cm^{-1}) on the C(111)-(1×1)-H surface is lower than that of a typical CH stretch mode of molecules in gas phase[28] [ν_{CH} ~2992 cm^{-1} for HCD_3, ~2893 cm^{-1} for $HC(CH_3)_3$, and 2887 cm^{-1} for $HC(CD_3)_3$][21]. This is believed to be due mainly to a change in the binding force although some difference can be attributed to the variation in reduced mass. Indeed, the bond between a hydrogen atom and a diamond surface carbon can have a very different charge distribution compared to a typical saturated CH bond.[18] Our thermal-desorption data yield a binding energy of 4.2 eV for H on C(111), which is about 10% less than a typical saturated hydrocarbon bond in a molecule. This is consistent with the lower mode frequency for H on C(111).

When dosing with atomic hydrogen onto the bare C(111) surface, saturation of H coverage was seen after ~10 min for the hot filament arrangement with 5×10^{-6} torr of H_2 in our chamber. Dosing of hydrogen onto the deuterium-terminated surface explicitly showed fast abstraction of D by H toward full coverage of H (Fig. 4). Similarly, an experiment starting with a fully H-terminated surface showed full conversion to the D-terminated surface upon dosing of D with a similar rate (not presented here as these spectra are similar). Recently, Thoms *et al.*[29] calculated the rates at room temperature using their high-resolution EELS data for adsorption of deuterium onto a bare diamond surface and a hydrogen-terminated surface. Their result gives a ratio of the two rates to be $K_{abs}/K_{ads}=0.05$, which would yield a saturated D coverage of $\Theta_D=0.95$. This can be compared with $\Theta_H=0.8$ obtained in the present measure-

ment. The roles of H and D should be interchangeable, and we expect the adsorption rates for the two isotope species to be comparable. The small difference in the reported saturation coverage may be due to experimental uncertainty and different sample dosing and preparation conditions. In any case, it is clear that, under the equilibrium condition, the saturation coverage for H atoms on C(111)-(1×1) is less than a monolayer on the substrate. The abstraction of the adsorbed D by the impinging H appears to be either direct (i.e., via the Eley-Rideal mechanism)[30,31] or by adsorption of H followed immediately by a reaction to form H_2 and then desorption of H_2 before the excited energy in the adsorbed H is dissipated away into the substrate.

Our result on thermal desorption of hydrogen from C(111)-(1×1) was analyzed with the usual theory for thermal desorption. It yields nearly first-order kinetics within the coverage range studied. This seems to contradict the fact that hydrogen desorbed from C(111) should appear in molecular form, and therefore the desorption kinetics should be second order. However, similar non-second-order thermal desorption has been observed for H desorption from Si surfaces. Sinniah *et al.* have measured a first-order desorption behavior of H from Si(100) and suggested that it may be due to irreversible excitations of adsorbed H atoms into delocalized band states before desorption.[32] There has also been experimental evidence of prepairing of H on Si(100), leading to possibly observed first-order desorption.[33] In other theoretical consideration, models based on H diffusion[34] and defect migration[35] on the Si surface to facilitate dihydride desorption have been proposed. Departures from second-order desorption have also been seen on Si(111)-(7×7) for low coverages; it is suggested that two binding sites may explain the behavior.[36] It is likely that thermal desorption of H from the diamond behaves similarly to that of H from silicon, recognizing the close analog of the two cases in many respects.

B. Reconstructed surface

Although the bare C(111)-(2×1)-reconstructed surface may not be of importance to the problem of CVD diamond growth, which typically involves a large amount of hydrogen-promoted (1×1) surface, its understanding is still of fundamental interest. This is particularly so because of close similarities between the equivalent Si, Ge, and α-Sn surfaces.

In their high-resolution EELS spectra for the reconstructed C(111)-(2×1) surface. Lee and Apai[4] observed spectral features at 92 (740 cm^{-1}) and 153 meV (1235 cm^{-1}) and attributed them to stretch and rock surface phonons. The assignment was reached by comparing[37,38] with scaled-up surface phonon frequencies of Si(111) using the same scaling factor relating the bulk phonon frequencies of Si(111) and C(111). The required electric-dipole character was known to come from the surface reconstruction. Our SFG spectra have much higher resolution than higher-resolution EELs, and we have observed two well-resolved bands at somewhat higher frequencies in the 1300–1550-cm^{-1} range. We note that they are still within the range of stretch surface phonon frequencies predicted by Lee *et al.*[4] from scaling. As we described in Sec. IV E, the low-frequency band seems to be associated with C—C bonds more inclined toward the surface normal, and the high-frequency band with C—C bonds more inclined toward the surface. Each band appears to have two split components (Fig. 6). We may find some understanding of the spectra by referring to the reconstructed surface structures depicted in Fig. 7.

The structures in Fig. 7 are derived from the Pandey π-bonded chain model, which has been widely accepted for the (2×1)-reconstructed surfaces.[6,16,23] There exist some variations of the model proposed by different researchers. In particular, buckling of the surface bilayer or dimerization of intrachain bonds that could reduce the configurational energy has been predicted. Bechstedt and Reichardt have concluded from a self-consistent, semiempirical tight-binding calculation that the Pandey π-bonded chain model with slight buckling but undimerized chains in the surface layer would have the lowest energy. On the other hand, recent work by Iarlori *et al.* predicted from a self-consistent *ab initio* molecular-dynamics calculation that there should be dimerized π-bonded chains with no buckling in the surface layer.

From the structures described in Fig. 7 and the required broken symmetry for SFG, we expect to see a surface phonon mode associated strongly with C—C bonds connecting the sublayers of the surface bilayer, and another with C—C bonds connecting the first two surface bilayers. It is known that the π-bonded chains of the top surface bilayer have strong sp^2 character, while the bonds connecting the top bilayer and the second bilayer have sp^2/sp^3 mixed character. Deeper into the bulk the bonds should have more and more sp^3 bulklike character. Raman measurements[19,39] on bulk diamond (sp^3), graphite (sp^2), and amorphous carbon (sp^2/sp^3) yielded bulk phonon frequencies of 1332.5, 1580, and 1360–1560 cm^{-1}, respectively. Studies of various hydrocarbon molecules[40] also showed that C—C bonds with sp^2 character have higher stretch frequencies than those with sp^3 character. We can therefore assign the high-frequency band ($\sim$1475 cm^{-1}) to surface phonons associated with the C—C bonds connecting the sublayers of the surface bilayer, and the low-frequency band ($\sim$1350 cm^{-1}) to phonons associated with the C—C bonds between the first and second surface bilayers. This result is consistent with the result deduced from the polarization dependence of the spectral peaks that the high- and low-frequency bands should be associated with bonds inclined, respectively, more toward the surface and more toward the surface normal.

Although we have made the general assignment of the high- and low-frequency bands, we still have to address the apparent splitting within each band. Of the two variations of the Pandey model, the one proposed by Bechstedt and Reichardt is the only one that can explain the fine structure. In this model, there are two different types of bonds within the top bilayer (high-frequency band) and also between the two top bilayers (low-frequency band) due to buckling. This leads to a splitting within each band. The general agreement our experimental results and the theoretical model lends credit to the model.

VI. CONCLUSION

We have studied the diamond C(111) surface dosed by atomic hydrogen using infrared-visible sum-frequency-generation (SFG) spectroscopy. The as-polished/dosed H-terminated surface spectra indicate a *single* monohydride peak (1331 and 2838 cm^{-1}) with an orientation preferentially along the surface normal. Atomic hydrogen is shown to be aggressive in hydrogen (deuterium) abstraction. Thermal-desorption spectroscopy of hydrogen suggests near first-order desorption with desorption energy of 4.0 eV. On the reconstructed (2×1) surface, CC features associated with the reconstruction of bilayers are readily observed at 1300–1500 cm^{-1}, showing two major bands confirming the Pandey π-bonded chain model.

ACKNOWLEDGMENTS

The work of R.P.C., J.Y.H., and Y.R.S. was supported by the Director, Office of Energy Research, Office of Basic Energy Sciences, Material Science Division of the U.S. Department of Energy under Contract No. DE-AC03-765F00098. R.P.C. acknowledges the support of a "1967 Science & Engineering Scholarship" of the Natural Sciences & Engineering Research Council of Canada and IBM for financial support. J.Y.H. acknowledges the support of a postdoctoral fellowship from IBM for financial support. T.J.C. acknowledges the support of NSC-R.O.C. under Contract No. NSC83-0208-M-001-094, and is grateful for the useful discussion with S. H. Lin, H. C. Chang, and J. C. Lin at IAMS.

[1]R. C. DeVries, Ann. Rev. Mater. Sci. **17**, 161 (1987); K. E. Spear, J. Am. Ceram. Soc. **72**, 171 (1989); J. C. Angus and C. C. Hayman, Science **241**, 913 (1988).

[2]Y. Cong, R. W. Collins, G. F. Epps, and H. Windischmann, Appl. Phys. Lett. **58**, 819 (1991).

[3]B. J. Waclawski, D. T. Pierce, N. Swanson, and R. J. Celotta, J. Vac. Sci. Technol. **21**, 368 (1982).

[4]S.-Tong Lee and G. Apai, Phys. Rev. B **48**, 2684 (1993).

[5]Takashi Aizawa, Toshihiro Ando, Mutsukazu Kamo, and Yoichiro Sato, Phys. Rev. B **48**, 18 348 (1993).

[6]A. V. Hamza, G. D. Kubiak, and R. H. Stulen, Surf. Sci. **206**, L833 (1988); **237**, 35 (1990); G. D. Kubiak, M. T. Schulberg, and R. H. Stulen, *ibid.* **277**, 234 (1992).

[7]Y. Mitsuda, T. Yamada, T. J. Chuang, H. Seki, R. P. Chin, J. Y. Huang, and Y. R. Shen, Surf. Sci. Lett. **257**, L633 (1991).

[8]R. P. Chin, J. Y. Huang, Y. R. Shen, T. J. Chuang, H. Seki, and M. Buck, Phys. Rev. B **45**, 1522 (1992).

[9]J. E. Butler (unpublished).

[10]Y. R. Shen, Nature (London) **337**, 519 (1989), and references therein.

[11]J. H. Hunt, P. Guyot-Sionnest, and Y. R. Shen, Chem. Phys. Lett. **133**, 189 (1987).

[12]P. Guyot-Sionnest, R. Superfine, J. H. Hunt, and Y. R. Shen, Chem. Phys. Lett. **144**, 1 (1988).

[13]X. D. Zhu, H. Suhr, and Y. R. Shen, Phys. Rev. B **35**, 3047 (1987).

[14]K. M. Gough, J. Chem. Phys. **91**, 2424 (1989).

[15]System based upon J. Y. Zhang, J. Y. Huang, Y. R. Shen, and C. Chen, J. Opt. Soc. Am. B **10**, 1758 (1993).

[16]B. B. Pate, Surf. Sci. **165**, 83 (1986).

[17]J. N. Smith, Jr. and W. L. Fite, J. Chem. Phys. **37**, 898 (1962).

[18]R. P. Chin, X. Blase, Y. R. Shen, and S. G. Louie (unpublished).

[19]S. A. Solin and A. K. Ramdas, Phys. Rev. B **1**, 1687 (1970).

[20]D. C. McKean, J. L. Duncan, and L. Batt, Spectrochim. Acta **29A**, 1037 (1973).

[21]J. K. Wilmshurst and H. J. Berstein, Can. J. Chem. **35**, 969 (1957).

[22]B. G. Koehler, C. H. Mak, D. A. Arthur, P. A. Coon, and S. M. George, J. Chem. Phys. **89**, 1709 (1988).

[23]K. C. Pandey, Phys. Rev. B **25**, 4338 (1982); D. Vanderbilt and S. G. Louie, *ibid.* **30**, 6118 (1984); F. Bechstedt and D. Reichardt, Surf. Sci. **202**, 58 (1988); G. D. Kubiak and K. W. Kalasinski, Phys. Rev. B **39**, 1381 (1989); S. Iarlori, G. Galli, F. Gygi, M. Parrinello, and E. Tosatti, Phys. Rev. Lett. **69**, 2947 (1992).

[24]H. Froitzheim, H. Lammering, and H. L. Gunter, Phys. Rev. B **27**, 2278 (1983).

[25]G. Vidali and D. R. Frankl, Phys. Rev. B **27**, 2480 (1983); G. Vadali, M. W. Cole, W. H. Weinberg, and W. A. Steele, Phys. Rev. Lett. **51**, 118 (1983).

[26]G. D. Kubiak and J. Butler (private communication).

[27]D. F. Edwards and H. R. Philipp, in *Handbook of Optical Constants of Solids,* edited by E. D. Polik (Academic, New York, 1985), p. 665; T. J. Chuang and J.-C. Lin (unpublished); H.-C. Chang, J.-C. Lin, J.-Y. Wu, and K.-H. Chen (unpublished).

[28]A. Kindness, D. C. McKean, and D. Stewart, J. Mol. Struct. **224**, 363 (1990), and references therein; G. Herzberg, *Infrared and Raman Spectra of Polyatomic Molecules* (Van Nostrand, Princeton, 1945); N. B. Colthup, L. H. Daly, and S. E. Wiberley, *Introduction to Infrared and Raman Spectroscopy* (Academic, New York, 1990).

[29]Brian D. Thoms, John N. Russell, Jr., Pehr E. Pehrsson, and James E. Butler, J. Chem. Phys. **100**, 8425 (1994).

[30]K. Christmann, *Introduction to Surface Physical Chemistry* (Springer, New York, 1991), pp. 203–213.

[31]W. Widdra *et al.*, Phys. Rev. Lett. **74**, 2074 (1995).

[32]K. Sinniah, M. G. Sherman, L. B. Lewis, W. H. Weinberg, J. T. Yates, and K. C. Janda, Phys. Rev. Lett. **62**, 567 (1989); J. Chem. Phys. **92**, 5700 (1990).

[33]John J. Boland, Phys. Rev. Lett. **67**, 1539 (1991); M. L. Wise, B. G. Koehler, P. Gupta, P. A. Coon, and S. M. George, Surf. Sci. **258**, 166 (1991).

[34]C. J. Wu, I. V. Ionova, and E. A. Carter, Surf. Sci. **295**, 64 (1993).

[35]P. Nachtigall, K. D. Jordan, and C. Sosa, J. Chem. Phys. **101**, 8073 (1994).

[36]G. A. Reider, U. Höfer, and T. F. Heinz, J. Chem. Phys. **94**, 4080 (1991).

[37]H. Ibach, Phys. Rev. Lett. **27**, 253 (1971); N. J. DiNardo, W. A. Thompson, A. J. Schell-Sorokin, and J. E. Demuth, Phys. Rev. B **34**, 3007 (1986); R. E. Schorder, R. J. Nemanich, and J. T. Glass, *ibid.* **41**, 3738 (1990); U. Harten, J. P. Toennies, and Ch. Woll, Phys. Rev. Lett. **57**, 2947 (1986).

[38]O. L. Alerhand, D. C. Allen, and E. J. Mele, Phys. Rev. Lett.

55, 2700 (1985); O. L. Alerhand and E. J. Mele, *ibid.* **59**, 657 (1987); Phys. Rev. B **37**, 2536 (1988); L. Miglio, P. Ruggerone, and G. Benedek, Phys. Rev. Lett. **62**, 3070 (1989); L. Miglio, P. Ruggerone, and G. Benedek, J. Electron Spectrosc. Relat. Phenom. **44**, 281 (1987); W. Goldammer and W. Ludwig, Phys. Lett. A **133**, 85 (1988); W. Goldammer, W. Ludwig, W. Zierau, and C. Falter, Surf. Sci. **141**, 139 (1984).

[39]S. Matsumoto, Y. Sato, M. Kamo, and N. Setaka, Jpn. J. Appl. Phys. **21**, L183 (1982).